

Results from an Analytical Investigation of Small-Scale Releases from Liquid Hydrogen Storage Systems

W. Winters¹ and W. Houf¹

1. Introduction

A need exists for developing codes and standards to support the wide-spread delivery of liquid hydrogen bulk fuel and fueling station storage. To develop these codes and standards the consequences of planned and unplanned hydrogen releases must be understood. The systems under consideration are mainly those used in supplying hydrogen for transportation. These systems include production storage tanks, tanker trucks and tanks located at vehicle fueling stations. Typically these systems store hydrogen in the saturated state at approximately 11 atmospheres. Storage vessels are heavily insulated and sometimes actively cooled to minimize the rate of hydrogen boil-off (intended hydrogen release).

This paper documents a series of models for describing an unintended slow leak or discharge from a liquid hydrogen (LH2) storage system. The first of these models is used to determine the state of flowing hydrogen as it exits a leak at atmospheric pressure. This model provides inlet conditions for a second model, a “plug flow” turbulent entrainment model that describes a region of initial entrainment and heating. In this region pure hydrogen enters and entrains enough air to bring the exiting hydrogen-air mixture to a temperature high enough to be analyzed using currently available thermodynamic models. Typically this temperature is approximately 65 K. The conditions exiting this zone of initial entrainment and heating are used as inlet conditions for a third model, a more conventional Gaussian turbulent entrainment jet or plume model that treats the hydrogen and air as a mixture of ideal gases. This third model is used to describe the trajectory and properties in most of the leak stream.

Unintended slow leaks from liquid hydrogen storage systems can occur from spaces containing either saturated vapor or a saturated liquid. Leaks occurring from the ullage volume in an LH2 storage tank or attached pressure relief vent lines or fittings represent leaks from the saturated liquid space. Leaks below the liquid level in an LH2 storage tank or leaks from liquid supply lines or fittings represent leaks from the saturated liquid space. These leaks are generally closer to ground level. Hydrostatic and liquid pumping pressure head may result in the liquid pressure levels being slightly higher than the saturation pressure at the liquid-vapor interface but in this study, these small pressure differences are assumed to be negligible. Depending on the storage pressure and leak location, leaks from LH2 systems can result in flashing two-phase flow as the hydrogen is exposed to atmospheric pressure.

¹ Sandia National Laboratory, Livermore, CA

Sandia is a multiprogram laboratory operated by Sandia Corporation, a Lockheed Martin Company, for the United States Department of Energy's National Nuclear Security Administration under Contract DE-AC04-94-AL85000.

The models discussed here assume that flashing hydrogen behaves as a simple compressible substance in thermodynamic equilibrium.

Thermodynamic models developed by NIST are used to calculate the state of leaking hydrogen and the state of hydrogen-air mixtures. NIST has incorporated its thermodynamic models into the program REFPROP [2] which can be used to generate tables and plots of thermodynamic and transport properties of important industrial fluids and their mixtures with an emphasis on hydrocarbons and refrigerants. While REFPROP is a stand-alone program, most of its subroutines are available in FORTRAN for linking into individual user applications. The models presented here have been cast into FORTRAN 95 programs that call the suite of REFPROP subroutines to model pure two-phase hydrogen and hydrogen mixtures with air.

REFPROP is based on the most accurate pure fluid and mixture models currently available. Three models are implemented for the thermodynamic properties of pure fluids. These include equations of state explicit in Helmholtz energy, the modified Benedict-Webb-Rubin equation of state and an extended corresponding states model. Mixture property calculations utilize a model that applies mixing rules to the Helmholtz energy of the mixture components. A departure function is used to account for the deviation from ideal gas mixing. Thermal conductivity and viscosity are modeled three different ways: fluid-specific correlations, an extended corresponding states method or the friction theory method.

In addition to describing the slow leak models, this paper presents computed results for leaks from an 11 atm liquid hydrogen storage system. Leaks from both the saturated vapor and saturated liquid spaces are considered.

2. Slow Leak Models

Figure 1 illustrates the two kinds of slow leaks that can occur from a system storing liquid hydrogen at a pressure P_s . Since hydrogen is stored at its saturation state, the hydrogen storage temperature T_s is equal to the saturation temperature corresponding to the storage pressure, *i.e.*:

$$T_s = T_{sat}(P_s) \quad (1)$$

For the system shown in Figure 1 leaks can occur from the saturated vapor space or saturated liquid space.

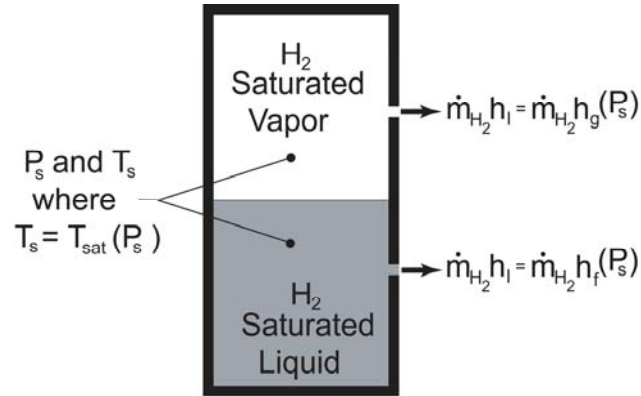


Figure 1. Leaks from LH₂ storage tank.

For a slow leak we make the following assumptions:

- Contents of the storage tank are at uniform pressure and temperature.
- Leak flows are quasi-steady.
- Hydrogen exits the leak at atmospheric pressure. In a slow leak through a microscopic crack the frictional pressure drop along the leak path is large. Hence it is reasonable to assume the exiting hydrogen is at or near atmospheric pressure.
- Potential and kinetic energy changes in the leaking flow stream are negligible. Slow leaks are by nature low velocity flows; hence it can be assumed that changes in kinetic energy are small when compared to enthalpy flux.
- Heat exchange between the containment and the leaking flow stream is negligible. The assumption of adiabatic flow becomes reasonable for leaks that have established themselves for a period of time. In such leaks solid material surrounding the leak has had sufficient time to equilibrate to a temperature that is nearly equal to the leak flow stream. Hence heat transfer from the containment to the exit stream is small when compared to the stream's enthalpy. The adiabatic assumption is conservative from the standpoint of safety since it leads to colder more dense exiting hydrogen streams. Plumes or jets having these starting conditions require longer distances to dilute to non-flammable levels.

In all the leak scenarios discussed here it is assumed that the ambient is composed of still air at atmospheric pressure (.10133 MPa) and temperature of 295 K.

Based on the above assumptions, the following steady flow energy equations can be written for saturated vapor and saturated liquid leaks:

$$\dot{m}_{H_2} h_l = \dot{m}_{H_2} h_g(P_s) \quad (2)$$

$$\dot{m}_{H_2} h_l = \dot{m}_{H_2} h_f(P_s) \quad (3)$$

where \dot{m}_{H_2} is the mass flow rate of hydrogen through the leak, h_l is the initial value of the hydrogen enthalpy as it enters the atmosphere, $h_g(P_s)$ is the enthalpy of saturated

hydrogen vapor at the storage pressure and $h_f(P_s)$ is the enthalpy of saturated hydrogen liquid at the storage pressure.

The transport of a slow leak through the atmosphere will be modeled using a series of three turbulent entrainment models. The models are shown schematically in Figure 2. The axial coordinate of the jet is designated by s and is in general a curved path influenced by gravity.

The three entrainment zones are:

Zone 1: Zone of initial entrainment and heating ($S_I = 0 \leq s \leq S_O$)

Zone 2: Zone of flow establishment ($S_O \leq s \leq S_E$)

Zone 3: Zone of established flow ($s \geq S_E$)

The pressure in all three zones is assumed to be atmospheric. This is an important requirement for the application of turbulent entrainment models.

In the first zone, “the zone of initial entrainment and heating”, pure hydrogen with a flow rate of \dot{m}_{H_2} and an enthalpy of h_I enters on the left ($s = 0$) at the leak exit plane. Air is entrained into the leak jet such that the temperature of the hydrogen-air mixture exiting the zone on the right ($s = S_O$) is T_O . T_O is assumed to be the lowest temperature for which the properties of a hydrogen-air mixture can be computed using available thermodynamic models. The model for the zone of initial entrainment and heating is described in Section 2.1.

The second zone, “the zone of flow establishment”, provides the transition between the zone of initial entrainment and heating and the zone of established flow. A uniform flow of hydrogen and air at one atmosphere and temperature T_O enters the zone on the left ($s = S_O$). In this zone the uniform flow profiles make a transition to Gaussian profiles characteristic of fully established jet flows before exiting on the right.

The third and by far the longest zone for the leak jet is “the zone of established flow.” In this zone the profiles for velocity and mixture properties vary with jet radius according to fully established Gaussian profiles that are constrained by the equation of state. The centerline values for velocity, hydrogen concentration and mixture enthalpy decrease with jet centerline distance. Furthermore the trajectory of the jet is influenced by buoyant forces due to local temperature and concentration differences.

The model for the zone of flow establishment and established flow are well known in the literature (see *e.g.* [3]) especially for liquid jets. They form the basis of a previous model developed by Houf and Schefer [4] to describe small-scale unintended releases of isothermal gaseous hydrogen. The present slow leak model for liquid hydrogen releases builds on this model by adding the energy equation so that buoyant forces resulting from the temperature difference between the cold jet and the ambient can be accounted for in

determining the trajectory of the jet. A separate model for the zone of initial entrainment and heating is used to overcome difficulties in accounting for multiphase hydrogen and air mixing and to provide thermodynamically consistent starting conditions for the zone of flow establishment.

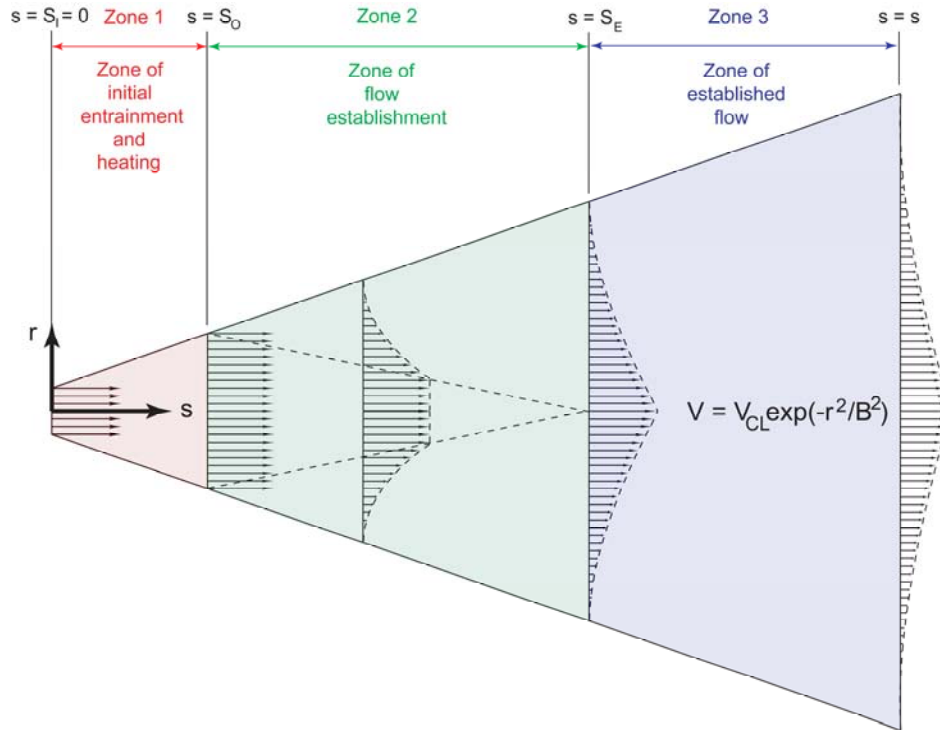


Figure 2. Flow zones for the complete turbulent entrainment model.

The three zones making up the turbulent entrainment model are discussed here in the context of slow leaks. However application of the three zones can also be made to fast leaks providing the leak stream has attained a pressure equal to the ambient pressure and changes in kinetic energy are small compared to the stream enthalpy.

2.1 Model for the Zone Of Initial Entrainment & Heating (Zone 1)

Table 1 shows saturation states for hydrogen generated from REFPROP [2]. The table indicates that the saturation temperature corresponding to .10133 MPa (1 atm) is 20.4 K. This suggests that hydrogen leak streams are likely to be quite cold. The model depicted by Figure 1 has been used to compute states for leaking hydrogen at one atmosphere. The actual temperature and quality of hydrogen brought from the storage pressure to one atmosphere in a constant enthalpy process (*i.e.* Equations 2 and 3) is shown in Figures 3 and 4. Exit quality varies over a wide range depending on whether the leak occurs from a saturated vapor space or a saturated liquid space; exit temperature varies only by a small amount. All slow leaks from the saturated liquid space result in two-phase flow at a temperature of 20.4 K. Leaks occurring from vapor spaces in systems that store hydrogen at approximately .7 MPa (~ 7 atm) or greater result in higher quality two-phase flows at

20.4 K. For storage pressures less than approximately .7 MPa (~ 7 atm) leaks from vapor spaces are superheated to temperatures slightly higher than 20.4 K.

Table 1. Saturation Table for Normal Hydrogen*

Temperature (K)	Pressure (MPa)	Liquid Density (kg/m ³)	Vapor Density (kg/m ³)	Liquid Enthalpy (kJ/kg)	Vapor Enthalpy (kJ/kg)	Liquid Entropy (kJ/kg-K)	Vapor Entropy (kJ/kg-K)
20.324	0.10000	70.901	1.3165	-0.44678	448.45	-0.021039	22.066
22.910	0.20000	67.714	2.4827	27.664	459.60	1.2122	20.066
24.683	0.30000	65.191	3.6465	49.883	463.14	2.0825	18.825
26.076	0.40000	62.951	4.8406	69.474	463.00	2.7927	17.884
27.243	0.50000	60.849	6.0867	87.664	460.42	3.4143	17.097
28.255	0.60000	58.802	7.4059	105.11	455.92	3.9828	16.399
29.154	0.70000	56.750	8.8235	122.27	449.66	4.5201	15.749
29.967	0.80000	54.633	10.374	139.54	441.57	5.0434	15.122
30.709	0.90000	52.383	12.111	157.35	431.39	5.5689	14.493
31.393	1.0000	49.890	14.128	176.35	418.48	6.1177	13.831
32.027	1.1000	46.944	16.619	197.73	401.43	6.7266	13.087
32.616	1.2000	42.962	20.136	224.80	376.13	7.4948	12.135

* Critical pressure = 1.2964 MPa, Critical temperature = 33.145 K

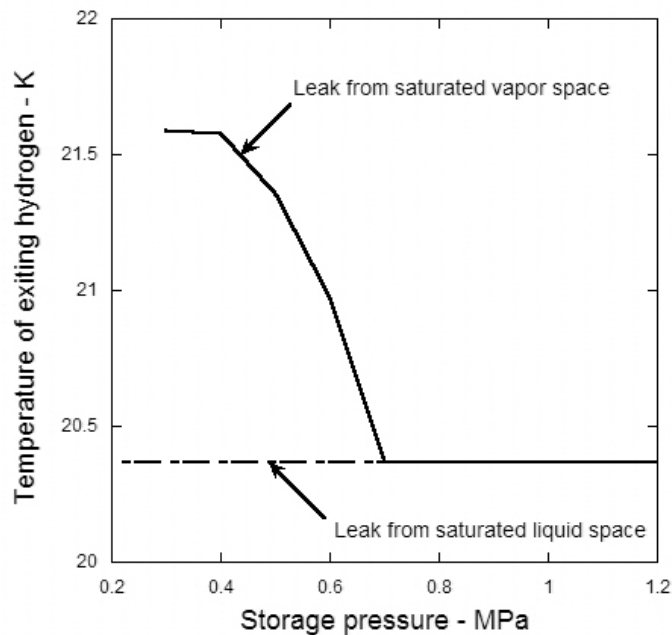


Figure 3. Temperature of exiting hydrogen as a function of storage pressure.

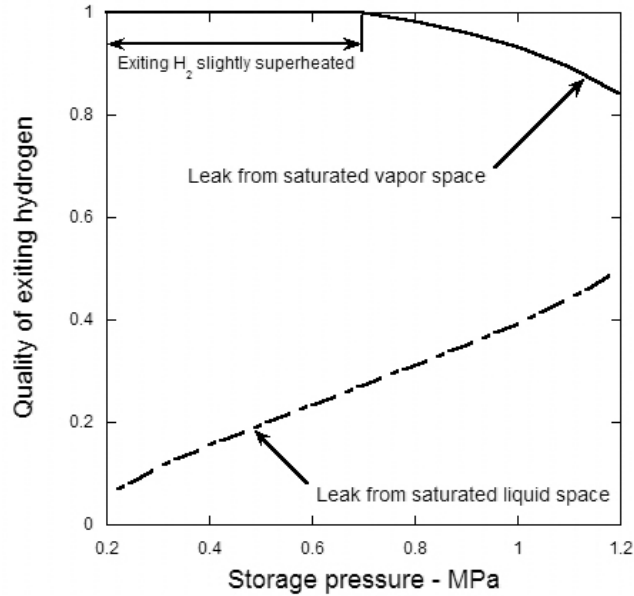


Figure 4. Quality of exiting hydrogen as a function of storage pressure.

It is clear that the thermodynamics of leaking hydrogen can be complicated considering it is likely to be a two-phase mixture at extremely low temperature. The thermodynamics become more difficult to describe as the exiting hydrogen stream entrains the surrounding ambient air. Near the exit any entrained air is likely to condense or even freeze resulting in a mixture that cannot be characterized by currently available equilibrium models. Even a comprehensive thermodynamic model such as REFPROP [2] cannot characterize mixtures in which two or more of the mixture species exist in the liquid phase. To overcome this difficulty, a “plug flow” turbulent entrainment model is used to model the first stage of the leaking hydrogen jet or plume. The following assumptions are used in developing a model for flow in zone 1, the zone of initial entrainment and heating:

- The jet flow is turbulent and quasi-steady
- Since the flow is fully turbulent and steady, radial molecular diffusion is neglected compared to radial turbulent transport. Radial turbulent transport is assumed to occur only at the jet periphery such that radial distributions of velocity concentration and enthalpy are uniform at any axial location in the jet, *i.e.* a plug-flow model is assumed.
- Streamwise turbulent transport is negligible compared to streamwise convective transport
- Buoyancy is neglected due to the fact that the zone of initial entrainment and heating is short and the trajectory of the jet is not significantly altered as a result of buoyant forces.
- Pressure is hydrostatic throughout the flow field and the thermodynamic pressure throughout the flow field is one atmosphere.
- The jet remains axisymmetric, *i.e.* there are no circumferential variations in velocity, enthalpy, density or concentration.
- The hydrogen and air are in thermodynamic equilibrium.
- Changes in kinetic and potential energy are negligible..

The entrainment model is schematically represented in Figure 5. The figure shows how continuity, momentum and energy are conserved in the zone of initial entrainment and heating. The exit temperature of the zone is an assumed value T_o . The exit temperature is arbitrary but modeling accuracy requires that this temperature be the lowest temperature where the exiting hydrogen-air mixture can exist as a gas (or the lowest temperature where REFPROP can compute the thermodynamic properties of the mixture). Keeping T_o low will also cause the zone of initial entrainment and heating to be short or even negligible compared to the remaining two zones that make up the leak jet. In the present study a value of 65 K was selected for T_o since it was the lowest temperature for which REFPROP could characterize the state for the exiting air-hydrogen mixture.

Figure 5a illustrates the conservation of mass for the zone. Pure hydrogen enters the zone on the left; air is turbulently entrained at the jet periphery and an air-hydrogen mixture exits on the right. The resulting continuity equation is:

$$\dot{m}_{H_2} + \dot{m}_A = \dot{m}_O. \quad (4)$$

Since the pressure throughout the flow field is uniform and the jet entrains stagnant air, the net pressure forces on the zone are zero and the entering and exit momentum is conserved in the zone resulting in the situation depicted in Figure 5b. The momentum equation for the zone is given by:

$$\dot{m}_{H_2} V_I = \dot{m}_O V_O. \quad (5)$$

where V_I is the velocity of hydrogen entering the zone (velocity at the leak plane) and V_O is the velocity of the air-hydrogen mixture exiting the zone.

Figure 5c illustrates conservation of energy for the zone. Pure hydrogen enters the zone at the left with a known enthalpy, h_I ; air is entrained at the known ambient enthalpy, h_{amb} and the air-hydrogen mixture exits the right at the enthalpy, h_o resulting in the following energy equation:

$$\dot{m}_{H_2} h_I + \dot{m}_A h_{amb} = \dot{m}_O h_o \quad (6)$$

where h_o is determined from the state specified by T_o , atmospheric pressure and the composition of the exiting air-hydrogen mixture. Using Equation (4), the energy equation can be rewritten as:

$$\dot{m}_{H_2} h_I + \dot{m}_A h_{amb} = (\dot{m}_{H_2} + \dot{m}_A) h_o \quad (7)$$

The entrained air, \dot{m}_A necessary to bring the exiting air-hydrogen mixture to a temperature of T_o at atmospheric pressure may be determined iteratively from Equation (7). Reference [3] describes the iterative process in detail and presents computed results for a number of leak scenarios.

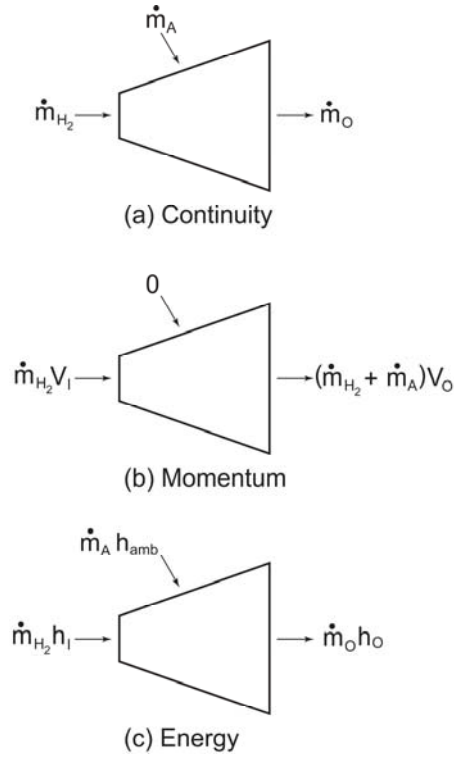


Figure 5. Model for the zone of initial entrainment and heating.

2.2 Gaussian Turbulent Entrainment Model (Zone 2 & Zone 3)

The modeling techniques outlined here for zones 2 and 3 have been developed by Gebhart *et. al.* [4] and many others. The assumptions used are similar to those outlined in Section 2.1 except that the flow is no longer a “plug flow” and the influence of buoyancy is included in determining the trajectory of the jet or plume.

The coordinate system used to describe jet trajectory and growth of the jet are shown in Figure 6. As mentioned previously, the jet axis lies along the streamwise s coordinate. The jet radial coordinate is r and the jet circumferential coordinate is ϕ . The angle between the jet axis and the x axis in the superimposed x - y - z Cartesian coordinate frame of Figure 6 is θ . The jet is assumed to be symmetrical about the x - y plane, hence the relationship between s , θ , x and y are given by:

$$\frac{dx}{ds} = \cos \theta \quad (8)$$

$$\frac{dy}{ds} = \sin \theta . \quad (9)$$

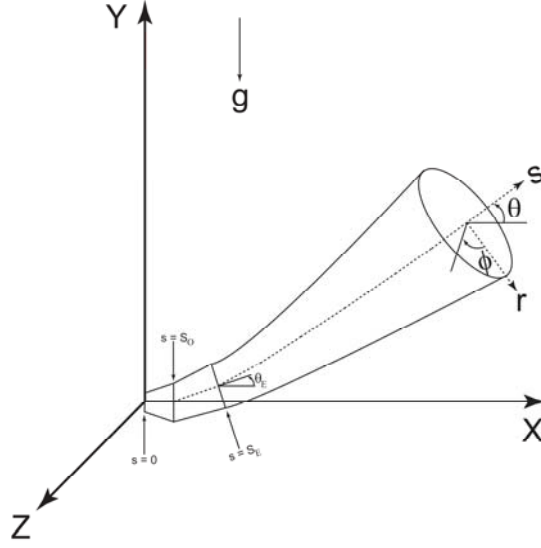


Figure 6. Coordinate system for buoyant jet.

The integral equations for jet continuity, the two components of momentum, hydrogen concentration, and energy may be summarized as follows:

$$\text{(continuity)} \quad \frac{\partial}{\partial s} \int_0^{2\pi} \int_0^{\infty} \rho V r dr d\phi = \rho_{amb} E \quad (10)$$

$$\text{(x-momentum)} \quad \frac{\partial}{\partial s} \int_0^{2\pi} \int_0^{\infty} \rho V^2 \cos \theta r dr d\phi = 0 \quad (11)$$

$$\text{(y-momentum)} \quad \frac{\partial}{\partial s} \int_0^{2\pi} \int_0^{\infty} \rho V^2 \sin \theta r dr d\phi = \int_0^{2\pi} \int_0^{\infty} (\rho_{amb} - \rho) g r dr d\phi \quad (12)$$

$$\text{(concentration)} \quad \frac{\partial}{\partial s} \int_0^{2\pi} \int_0^{\infty} \rho V Y r dr d\phi = 0 \quad (13)$$

$$\text{(energy)} \quad \frac{\partial}{\partial s} \int_0^{2\pi} \int_0^{\infty} V \rho (h - h_{amb}) r dr d\phi = 0 \quad (14)$$

where ρ , V , h , Y , g , and h_{amb} are the jet density, velocity, enthalpy, hydrogen mass fraction, gravitational constant and ambient enthalpy respectively. The ambient properties outside the jet are designated with the subscript “*amb*”. (“*amb*” is equivalent to the state “*A*” in the previous subsection.)

A number of investigators including Albertson *et. al.* [5] and more recently Houf and Schefer [6] have shown that within the zone of established flow, the mean velocity profiles are nearly Gaussian and take the form

$$V = V_{CL} \exp(-r^2 / B^2) \quad (15)$$

where V_{CL} is the local centerline velocity, r is the radial coordinate and B is the characteristic jet width or the radial distance at which V is equal to $1/e$ times V_{CL} . Fan [7], Hoult *et. al.* [8] and others have shown that scalar profiles within the jet are also Gaussian and can be expressed as:

$$\rho - \rho_{amb} = (\rho_{CL} - \rho_{amb}) \exp\left(\frac{-r^2}{\lambda^2 B^2}\right) \quad (16)$$

$$\rho Y = \rho_{CL} Y_{CL} \exp\left(\frac{-r^2}{\lambda^2 B^2}\right) \quad (17)$$

where ρ_{CL}, Y_{CL} are the local centerline density and hydrogen mass fraction respectively. The parameter λ is discussed below.

The selection of a radial profile for h must be constrained in such a way as to satisfy the equation of state for the hydrogen air mixture. If reference enthalpies for each component are assigned a value zero at a temperature of zero, it follows that

$$h = C_p T \quad (18)$$

where C_p is the mixture specific heat. Here we assume the hydrogen-air mixture behaves as a calorically perfect ideal gas (specific heats of air and hydrogen have a negligible variation due to temperature).

For a mixture of ideal gases it follows that

$$T = \frac{P_{amb} M}{\rho \bar{R}} \quad (19)$$

where M is the mixture molecular weight and \bar{R} is the universal gas constant.

Substituting (2.24) into (2.23) yields

$$h = \frac{C_p P_{amb} M}{\rho \bar{R}}. \quad (20)$$

The mixture specific heat and molecular weight can be expressed as

$$C_p = Y C_{p_{H_2}} + (1-Y) C_{p_A} \quad (21)$$

$$M = \left[\frac{Y}{M_{H_2}} + \frac{1-Y}{M_A} \right]^{-1} \quad (22)$$

where $C_{p_{H_2}}$ and C_{p_A} are the specific heats of hydrogen and air and M_{H_2} and M_A are the molecular weights.

The radial distribution in h can be determined by combining Equations (16-17), (2.25), (20-22). This complicated expression is represented here as

$$h = f(\rho_{CL}, Y_{CL}, B, r). \quad (23)$$

The parameter λ in the radial distribution functions (Equations 16,17) represents the relative spreading ratio between velocity and scalar properties ρ , Y and h . This spreading ratio is related to the turbulent entrainment Prandtl and Schmidt number effects.

Since the jet is assumed to be axisymmetric, there are no variations in ϕ and the Gaussian profiles given by Equations (15-17) may be substituted into the integral Equations (10-13) and integrated to yield the following ordinary differential equations:

$$\text{(continuity)} \quad \frac{d}{ds} \left\{ V_{CL} B^2 \left[\rho_{amb} - \frac{\lambda_\rho^2}{(\lambda_\rho^2 + 1)} (\rho_{amb} - \rho_{CL}) \right] \right\} = \frac{\rho_{amb} E}{\pi} \quad (24)$$

$$\text{(x-mom.)} \quad \frac{d}{ds} \left\{ V_{CL}^2 B^2 \cos \theta \left[\rho_{amb} - \frac{2\lambda_\rho^2}{(2\lambda_\rho^2 + 1)} (\rho_{amb} - \rho_{CL}) \right] \right\} = 0 \quad (25)$$

$$\text{(y-mom.)} \quad \frac{d}{ds} \left\{ V_{CL}^2 B^2 \sin \theta \left[\frac{\rho_{amb}}{2} - \frac{\lambda_\rho^2}{(2\lambda_\rho^2 + 1)} (\rho_{amb} - \rho_{CL}) \right] \right\} = (\rho_{amb} - \rho_{CL}) \lambda_\rho^2 B^2 g \quad (26)$$

$$\text{(concentration)} \quad \frac{d}{ds} [V_{CL} B^2 (\rho_{amb} Y_{amb} - \rho_{CL} Y_{CL})] = 0 \quad (27)$$

The energy Equation (14) reduces to

$$\text{(energy)} \quad \frac{\partial}{\partial s} \left\{ 2\pi \int_0^\infty V \rho (h - h_{amb}) r dr \right\} = 0. \quad (28)$$

In Equation (28), V , ρ and h , are replaced by their Gaussian profiles from Equations (15), (16) and (23) respectively. The final form of this integral equation is not shown here. Equations (8-9), (24-28), represent a system of 7 ordinary differential equations and algebraic equations and 7 unknowns (x , y , θ , B , ρ_{CL} , V_{CL} , and Y_{CL}). COLDPLUME [3], a Fortran 95 computer program was written to solve this system of equations and predict the behavior of atmospheric pressure leaks from LH2 systems. The differential-algebraic solver DDASKR [9] was used in solving the equations. DDASKR is an improved version of the differential/algebraic system solver DASSL [10].

COLDPLUME solves the integral in Equation (28) numerically using the trapezoidal rule. Typically, the upper integration limit ∞ is replaced by $3B$ and 1000 equally spaced intervals (dr) are used to perform the integration. Numerical experiments were conducted in which the upper limit of integration was increased to $5B$ and 10,000 equally spaced intervals were used. The computed values for the seven dependent variables were unaffected in the first four significant figures.

A model for zone 2, the zone of flow establishment is used to compute the initial values of the dependent variables (e.g. initial centerline values for density, velocity, mass fraction, enthalpy, etc.). This model which was originally proposed by Gebhart *et. al.* [4] and Abraham [11]. Detailed documentation is provided in reference [3].

In order to complete the Gaussian turbulent entrainment model, a model for the entrainment, E in Equation (24) must be proposed. In the absence of data for the entrainment of air into cold hydrogen jets, COLDPLUME utilizes the entrainment model

of Houf and Schefer [6] which is based on an approach suggested by Hirst [12]. The Houf and Schefer entrainment model has been experimentally verified for hydrogen jets at ambient temperature. Reference [3] contains a detailed description of the entrainment model.

3.0 Results

COLDPLUME predictions were compared to isothermal plume calculations made using the Houf and Schefer turbulent entrainment plume model [6]. When COLDPLUME is run with an initial hydrogen temperature equal to the ambient temperature, the predicted jet behavior is identical to that predicted by Houf and Schefer.

The slow leaks presented here are valid for a liquid hydrogen storage pressure of 11 atm absolute. This pressure is typical of systems used in the industry. It is important to note that leaks from systems at other storage pressures may behave differently since the initial storage pressure impacts the state of hydrogen as it is brought to atmospheric pressure at the leak plane. It is this state that provides the starting condition for the turbulent entrainment models that describe the trajectory and properties of the leak stream.

The trajectory for a series of leaks from the saturated vapor space is shown in Figure 7. Figure 8 contains a similar plot for a series of leaks from the saturated liquid space. The curves in Figures 7 and 8 represent the centerline of the jet plotted in x and y coordinates that are normalized by the leak diameter, D_l . In all cases a leak diameter of 1 mm was used and the jet angle was assumed to be zero such that the centerline of the jet at the origin aligns with the x axis. The locations where the centerline concentration of hydrogen (mole fraction) fall to 8, 6, 4 and 2 percent are shown for each trajectory plotted.

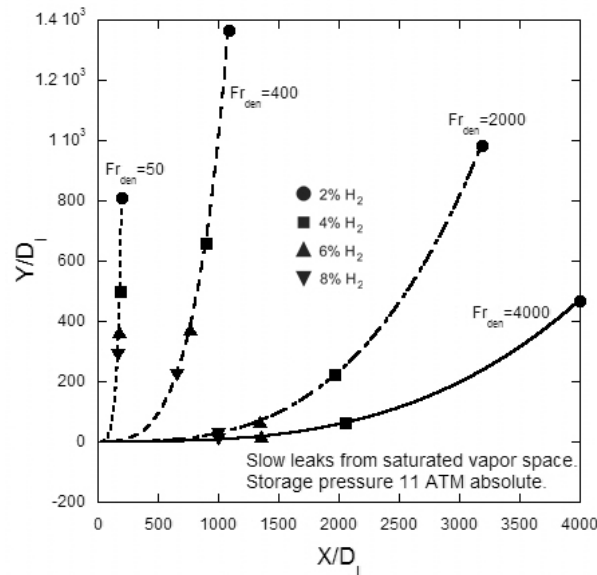


Figure 7. Trajectories for slow leaks from the saturated vapor space.

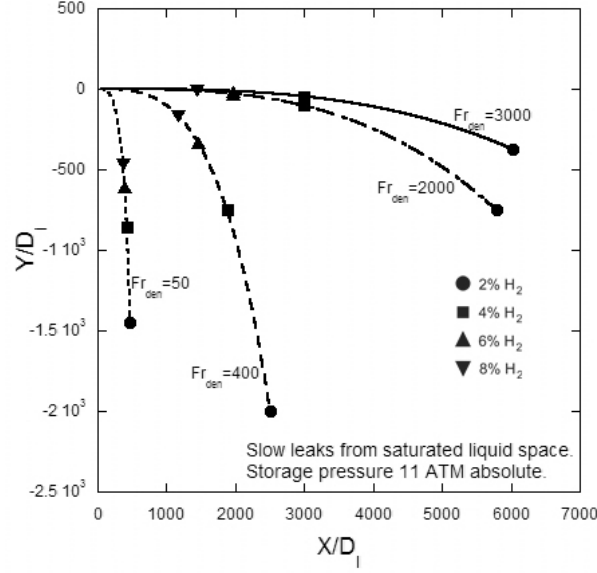


Figure 8. Trajectories for slow leaks from the saturated liquid space.

Following the procedure of Houf and Schefer [6], slow leaks are characterized with the leak densimetric Froude number

$$Fr_{den} = V_l / \sqrt{gD_l |\rho_{amb} - \rho_l| / \rho_l} \quad (29)$$

where V_l , D_l , ρ_l , ρ_{amb} and g are the hydrogen leak velocity, leak diameter, hydrogen leak density, ambient air density and gravitational constant respectively. The density ratio $|\rho_{amb} - \rho_l| / \rho_l$ depends on the storage pressure, ambient pressure, ambient temperature and whether the leak occurs from the saturated vapor space or the saturated liquid space. For a storage pressure of 11 atm, an ambient pressure of 1 atm and an ambient temperature of 295 K, the densimetric Froude number can be simplified as:

$$\text{Leaks from Saturated Vapor Space: } Fr_{den} = 2.333V_l / \sqrt{gD_l} \quad (30)$$

$$\text{Leaks from Saturated Liquid Space: } Fr_{den} = 1.304V_l / \sqrt{gD_l} \quad (31)$$

The densimetric Froude number is a measure of how the initial jet momentum influences the trajectory of the jet. For large Froude numbers, the jet is more momentum-driven resulting in a jet trajectory that aligns more closely with the original axis of the jet, in this case, the x axis. At low Froude numbers the jet trajectory is strongly influenced by buoyancy forces causing the jet to quickly bend upward or downward depending on whether the jet is positively or negatively buoyant. The influence of Froude number is clearly evident in Figures 7 and 8.

Starting conditions for all COLDPLUME calculations are derived from the plug flow entrainment model described in Section 2.1. The temperature and pressure of the hydrogen-air mixture exiting the zone of initial entrainment and heating are 65 K and 1 atm respectively. For leaks occurring from the saturated vapor space the density of this mixture is less than that of ambient air causing all leaks to be positively buoyant. This results in the upward trajectories shown in Figure 7. For leaks occurring from the saturated liquid space the density of the air-hydrogen mixture at 65K and 1 atm is greater

than the ambient air causing the leaks to be negatively buoyant with trajectories bending downward as shown in Figure 8.

COLDPLUME was used to generate Tables 2 and 3 showing the maximum radial distance from the leak origin ($s = S_l = 0$) to a point on the leak-jet trajectory curve where the hydrogen mole fraction concentrations are 2%, 4%, 6% and 8%. These tables are similar to the one generated by Houf and Schefer [6] for ambient temperature leaks of hydrogen gas. All LH2 leaks are assumed to occur from storage systems containing saturated liquid hydrogen at 11 atm absolute pressure. Table 2 shows radial distances for leaks from the saturated vapor space. Radial distances for leaks from the saturated liquid space are shown in Table 3. Because it was assumed (see Section 2.1) that leaking hydrogen expands adiabatically from the tank interior to the leak plane, the distances shown in Tables 2 and 3 represent conservative (*i.e.* longest possible) predictions. Furthermore it is assumed that the leak jet or plume is allowed to penetrate the atmosphere unimpeded by obstructions or by the ground.

Froude number ranges given in Tables 2 and 3 vary from very low values where the jets are strongly influenced by buoyancy to large Froude numbers where buoyancy has little influence and the leaks approach choked flow. Choked flows cannot be analyzed directly with turbulent entrainment models since the leak stream is no longer at atmospheric pressure. Several pseudo source models have been proposed in order to facilitate the use of turbulent entrainment models in the analysis leaks with extremely high flow rates. See *e.g.* references [3,13].

Table 2. Maximum radial distances from leak origin to hydrogen mole fractions of 2%, 4%, 6% and 8% for various leak densimetric Froude numbers and leak angles between $\pm 90^\circ$. Leaks are from saturated vapor space in 11 atm LH2 tank.

$(Fr_{den})^1$	$(R/D)_{max}$ 2%	$(R/D)_{max}$ 4%	$(R/D)_{max}$ 6%	$(R/D)_{max}$ 8%
10	479	314	245	204
50	883	570	438	361
100	1134	720	546	445
200	1143	899	670	540
400	1812	1112	849	692
600	2053	1293	974	780
800	2241	1443	1072	855
1000	2500	1581	1173	937
2000	3333	1985	1343	996
3000	3799	2047	1352	998
4000	4023	2061	1354	998
5000 ²	4111	2063	1354	998

1 $Fr_{den} = 2.233 V_l / (g D)^{1/2}$

2 Larger Froude numbers result in choked flow.

Table 4. Maximum radial distances from leak origin to hydrogen mole fractions of 2%, 4%, 6% and 8% for various leak densimetric Froude numbers and leak angles between $\pm 90^\circ$. Leaks are from saturated liquid space in 11 atm LH2 tank.

$(Fr_{den})^1$	$(R/D)_{max}$ 2%	$(R/D)_{max}$ 4%	$(R/D)_{max}$ 6%	$(R/D)_{max}$ 8%
10	881	573	442	367
50	1610	1022	775	631
100	2051	1276	950	766
200	2483	1573	1197	975
400	3207	2024	1498	1188
600	3768	2334	1710	1362
800	4293	2658	1900	1433
1000	4842	2875	1948	1445
2000	5838	2990	1965	1449
3000 ²	6038	2999	1966	1449

1 $Fr_{den} = 1.304 V_l / (g D)^{1/2}$

2 Larger Froude numbers result in choked flow.

Use of Tables 2 and 3 can be illustrated by a simple example. Let us determine the radial distance between the leak source and a point on the centerline of the leak stream where the mole fraction of hydrogen has dropped to 4%. We shall assume the leak diameter is 1 mm with a leak velocity corresponding to a densimetric Froude number of 1000. Table 2 indicates that the radial distance for a saturated vapor leak is 1.581 m. Table 3 indicates a distance of 2.875 m for a saturated liquid leak. Comparing these distances to the distances computed by Houf and Schefer [6] for ambient temperature hydrogen leaks, we find that for the saturated vapor leak the distance is more than 4 times greater; for the saturated liquid leak the distance is more than 7 times greater. Note that we have used the densimetric Froude number as a basis for comparing the three leaks. Table 4 shows radial distances for the three leaks using the mass flow rate as a basis of comparison. The saturated vapor and saturated liquid leaks are for a storage tank at 11 atm absolute pressure and all three leaks are for a leak diameter, $D_l = 1$ mm and a mass flow rate of .027 g/s. The table shows that for the 4% radial distance the saturated vapor leak is approximately 3 times greater than the ambient temperature leak distance; the saturated liquid leak the distance is approximately 3.6 times greater than the ambient temperature leak distance. Hence regardless of whether mass flow rate or Froude number is used as a basis for comparing the three leaks, saturated vapor and saturated liquid hydrogen leaks require considerably longer distances to dilute the leak stream.

Table 4. Comparison of three slow leak all having a mass flow rate of .027 g/s and a leak diameter of 1 mm. LH2 leaks are from an 11 atm tank.

Type of Leak	(Fr_{den})	$(R/D)_{max}$ 2%	$(R/D)_{max}$ 4%	$(R/D)_{max}$ 6%	$(R/D)_{max}$ 8%
Ambient leak	1000	765	379	250	185
Sat. Vapor Leak	94.4	1828	1166	888	719
Sat. Liquid leak	37.8	2163	1359	1032	844

For liquid hydrogen storage systems leaking hydrogen is extremely cold (approximately 20 K) and multi-phased resulting in densities that are considerably higher than ambient temperature hydrogen. As a result, greater distances are required to dilute the leak stream.

In their study of ambient temperature hydrogen leaks, Houf and Schefer [6] showed that for momentum dominated jets, hydrogen dilution distances are independent of the jet densimetric Froude number. Figures 9 and 10 demonstrate that the same is true for saturated vapor and liquid leaks. Each figure shows how the reciprocal of hydrogen mole fraction, $1/X$ varies along the centerline of jets having varying Froude numbers. The distance along the jet centerline is normalized by the leak diameter, D_l .

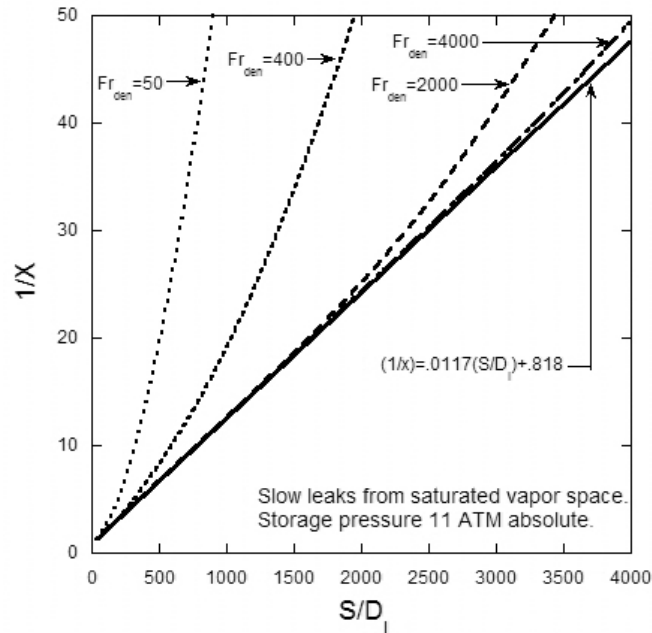


Figure 9. Dilution profiles for saturated vapor leaks from an 11 atm storage tank.

For increasing Froude numbers the relationship between $1/X$ and S/D_l approaches a straight line, *i.e*

$$\text{High } Fr_{den} \text{ leaks from vapor space: } \frac{1}{X} = .0117 \left(\frac{S}{D_l} \right) + .818 \quad (32)$$

$$\text{High } Fr_{den} \text{ leaks from liquid space: } \frac{1}{X} = .00806 \left(\frac{S}{D_l} \right) + .827 \quad (33)$$

Equations (32) and (33) provide a simple way for estimating hydrogen dilution distances for momentum nominated jets.

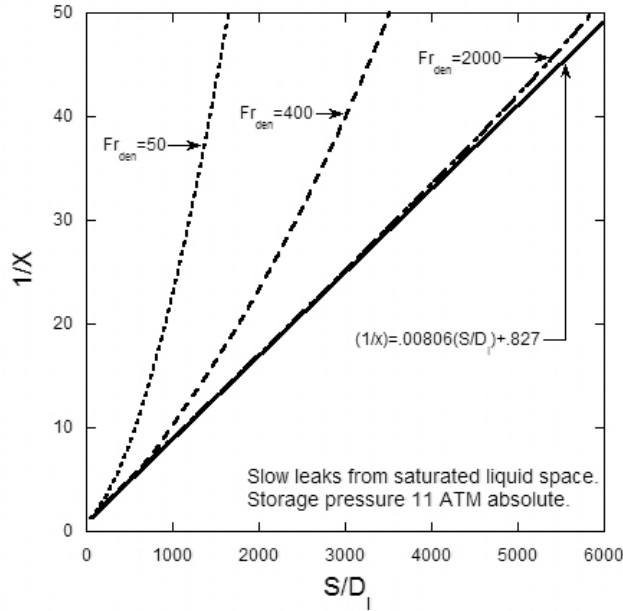


Figure 10. Dilution profiles for saturated liquid leaks from an 11 ATM storage tank.

4.0 Summary and Conclusions

A series of turbulent entrainment models have been used to predict the characteristics of leaking jets or plumes that result from unintended slow releases of hydrogen from liquid hydrogen storage systems. Equilibrium thermodynamic models based on the NIST REFPROP subroutines are used to predict hydrogen and hydrogen-air states as the leak stream is decompressed from tank storage conditions to atmospheric pressure and a temperature of 65 K. This transition is modeled as a two step process. In the first step pure hydrogen (either saturated vapor or saturated liquid at the tank pressure) is decompressed adiabatically to atmospheric pressure. The adiabatic assumption is conservative from the standpoint of safety since it leads to colder more dense hydrogen leak streams. In the second step a plug flow turbulent entrainment model is used to model a zone of initial entrainment and heating. Pure hydrogen enters this zone and entrains enough ambient temperature air to bring the leak stream to 65 K. This temperature is the lowest temperature for which existing thermodynamic equilibrium models can be used to compute air-hydrogen state points. It is also a temperature that is high enough for the atmospheric pressure hydrogen-air mixture to be treated as a mixture of ideal gases. This mixture provides the starting point for further turbulent entrainment model calculations. For these calculations the leak stream radial profiles for velocity, density, concentration and enthalpy are assumed to be Gaussian. This Gaussian turbulent entrainment model has been developed into the computer code COLDPLUME that can be used to predict the behavior of the longest part of the leak stream. COLDPLUME accounts for both thermal and solutal buoyancy effects. The model used to predict the rate of ambient air entrainment for the plug flow and COLDPLUME models was developed by Houf and Schefer [6]. This model has been experimentally validated for ambient temperature hydrogen leaks. To the author's knowledge, no experimentally validated entrainment rate model currently exist for low temperature hydrogen.

The models described above were used to predict the characteristics of slow leaks from the saturated vapor and saturated liquid spaces of an 11 atm liquid hydrogen storage tank. An absolute pressure of 11 atm is typical for current liquid hydrogen storage systems. Tables have been constructed to show distances required to dilute leak streams to hydrogen mole fractions (volume fractions) of 8, 6, 4, and 2%. Simple expressions have been developed to describe dilution distances for momentum dominated jets. Predictions show that vapor leaks are positively buoyant and tend to flow upward in still air. Leaks from the saturated liquid space are negatively buoyant and tend to flow downward toward the ground. Leaks from liquid hydrogen storage systems have relatively high densities when compared to ambient temperature hydrogen leaks. As a result dilution distances for LH2 leaks tend to be several times greater than distances for ambient temperature hydrogen leaks.

5.0 Acknowledgements

This work was supported by the U. S. Department of Energy, Office of Energy Efficiency and Renewable Energy under the Codes and Standards subprogram element managed by Antonio Ruiz.

6.0 References

- [1] W. Peschka, "State of Hydrogen Cryofuel Technology for Internal Combustion Engines," *Hypothesis Conference*, Grimstad, Norway, August 1997.
- [2] E. W. Lemmon, M. L. Huber, M. O. McLinden, "NIST Reference Fluid Thermodynamic and Transport Properties-REFPROP," Version 8 User's Guide, U. S. Department of Commerce Technology Administration, National Institute of Standards and Technology, Standard Reference Data Program, Gaithersburg, Maryland 20899, April, 2007.
- [3] W. S. Winters, "Modeling Leaks from Liquid Hydrogen Storage Systems," SAND2009-0035, Sandia National Laboratories, Livermore, CA, January 2009.
- [4] B. Gebhart, D. S. Hilder and M. Kelleher, "The Diffusion of Turbulent Buoyant Jets," *Advances in Heat Transfer*, Vol. 16, Academic Press, Inc., Orlando, Florida, 1984.
- [5] M. L. Albertson, Y. B. Dai, R. A. Jensen and H. Rouse, "Diffusion of Submerged Jets," *Transactions of the American Society of Civil Engineers*, Vol. 115, pp 639-697, 1950.
- [6] W. Houf, R. Schefer, "Analytical and Experimental Investigation of Small-Scale Unintended Releases of Hydrogen," *International Journal of Hydrogen Energy*, Vol. 33, pp 1435-1444, 2008.
- [7] L. H. Fan, "Turbulent Buoyant Jets into Stratified and Flowing Ambient Fluids," Rep. No. KH-R-15, W. M. Keck Laboratory, California Institute of Technology, Pasadena, 1967.

- [8] D. P. Hoult, J. A. Fay, and L. J. Forney, "A Theory of Plume Rise Compared with Field Observations," Journal of Air Pollution Control Association, Vol. 19, 585-590, 1969.
- [9] L. R. Petzold, P. N. Brown, A. C. Hindmarsh, and C. W. Ulrich, "DDASKR – Differential Algebraic Solver Software," Center for Computational Science & Engineering, L-316, Lawrence Livermore National Laboratory, P.O. Box 808, a private communication with L. R. Petzold.
- [10] L. R. Petzold, "A Description of DASSL: A Differential/Algebraic Solver System Solver," SAND82-8637, Sandia National Laboratories, Livermore, CA, September, 1982.
- [11] G. Abraham, "Horizontal Jets in Stagnant Fluid of Other Density," J. Hydraul. Div.Am.Soc.Civ.Eng. Vol. 9, 1965
- [12] E. A. Hirst, "Analysis of Buoyant Jets within the Zone of Flow Establishment," Oak Ridge National Laboratory Report, ORNL-TM-3470, 1971.
- [13] A. D. Birch, D. J. Hughes, and F. Swaffield, "Velocity Decay of High Pressure Jets," Combustion Science and Technology, Vol. 36, 1987.